Surface Properties of Poly(3-hydroxybutyrate-co-3- hydroxyvalerate) Banded Spherulites Studied by Atomic Force Microscopy and Time-of-Flight Secondary Ion Mass Spectrometry

ARTICLE *in* LANGMUIR · JULY 2003

Impact Factor: 4.46

3 AUTHORS, INCLUDING:

Jun Xu
Tsinghua University
84 PUBLICATIONS **1,229** CITATIONS
SEE PROFILE

Lin Li
Beijing Normal University
212 PUBLICATIONS **5,639** CITATIONS
SEE PROFILE

Surface Properties of Poly(3-hydroxybutyrate-*co*-3-hydroxyvalerate) Banded Spherulites Studied by Atomic Force Microscopy and Time-of-Flight Secondary Ion Mass Spectrometry

Yong Jiang,[†] Jian-Jun Zhou,[†] and Lin Li*

State Key Laboratory of Polymer Physics and Chemistry, Center for Molecular Science, Institute of Chemistry, Chinese Academy of Sciences, Beijing 100080, China

Jun Xu,[‡] Bao-Hua Guo,[‡] Zeng-Min Zhang,[‡] Qiong Wu,[§] and Guo-Qiang Chen[§]

Institute of Polymer Science & Engineering, Department of Chemical Engineering, School of Materials Science and Engineering, and Department of Biological Sciences & Biotechnology, Tsinghua University, Beijing 100084, China

Luo-Tao Weng,[||] Zhuo-Lin Cheung,[⊥] and Chi-Ming Chan*[,⊥]

Materials Characterization and Preparation Center and Department of Chemical Engineering, Hong Kong University of Science and Technology, Clear Water Bay, Hong Kong

Received May 19, 2003. In Final Form: June 30, 2003

Banded spherulites of poly(3-hydroxybutyrate-*co*-3-hydroxyvalerate) (P(3HB-3HV)) random copolymer were prepared by isothermal crystallization at 90 °C for 10 h. Using tapping-mode atomic force microscopy (AFM), the concentric periodic ridges and valleys on the surface of the banded spherulites of this polymer were found to consist of edge-on and flat-on lamellae, respectively. The periodic concentric ridges and valleys observed by AFM corresponded to the periodic extinction rings observed by polarized optical microscopy. AFM measurements showed that the interaction between the AFM probe and the sample surface can be significantly influenced by lamellar orientation.

Introduction

Poly[(*R*)-3-hydroxybutyrate] (P(3HB)) and its derivative, poly(hydroxyalkanoate)s (PHAs), are produced by a variety of bacteria.[1−4] The degradability of these natural polymers leads to potential applications in many environmentally sensitive areas. In particular, the biodegradability of PHAs has been evaluated in various natural environments.[5] The enzymatic degradation of PHAs has been extensively studied using either solution-cast films[6−8] or melt-crystallized films.[9−12] It has been reported that the crystalline region plays an important role in the degradation behavior. Usually, the degradation of the polymer initially occurs in the amorphous regions and subsequently develops into the crystalline phase. The degradation rate was found to be strongly affected by the degree of crystallinity and morphology. It has been known that banded spherulites of PHA films may form during crystallization from the melt at different temperatures, attributing to the regular twisting of the radial crystallite ribbons during their growth along the crystal axis.[13,14]

Other surface properties, such as surface morphology and chemical composition, may also influence the degradation behavior. Atomic force microscopy (AFM) has been widely used to image surface topography on a nanometer scale and to measure chemical, adhesive, and elastic properties. Several previous studies have successfully used AFM to quantify the elastic properties, using either the force modulation[15−17] or indentation modes.[18,19] Lateral force microscopy (LFM), force-distance curve

* To whom correspondence should be addressed. Email address: lilin@iccas.ac.cn.

[†] Present address: Graduate School of the Chinese Academy of Sciences.

[‡] Institute of Polymer Science & Engineering, Department of Chemical Engineering, School of Materials Science and Engineering, Tsinghua University.

[§] Department of Biological Sciences & Biotechnology, Tsinghua University.

[||] Materials Characterization and Preparation Center, Hong Kong University of Science and Technology.

[⊥] Department of Chemical Engineering, Hong Kong University of Science and Technology.

(1) Holmes, P. A. *Developments in crystalline polymers*; Bassett, D. C., Ed.; Elsevier: Amsterdam, 1988; Vol. 2.

(2) Hammond, T.; Liggat J. J. *Degradable Polymers: Principles and Applications*; Scott, G., Gilead, D., Eds.; Chapman and Hall: London and New York, 1995; Chapter 5, p 88.

(3) Anderson, A. J.; Dawes, E. A. *Microbiol. Rev.* **1990**, *54*, 450.

(4) Doi, Y.; Kitamura, S.; Abe, H. *Macromolecules* **1995**, *28*, 4822.

(5) Doi, Y. *Microbial Polyesters*; VCH Publishers: New York, 1990.

(6) Doi, Y.; Kanesawa, Y.; Kunioka, M.; Saito, T. *Macromolecules* **1990**, *23*, 26.

(7) Shimomura, E.; Scandola, M.; Doi, Y. *Macromolecules* **1994**, *27*, 4429.

(8) Abe H, Matsubara I, Doi, Y. *Macromolecules* **1995**, *28*, 844.

(9) Kumagai, Y.; Kanesawa, Y.; Doi, Y. *Makromol. Chem.* **1992**, *193*, 53.

(10) Tomasi, G.; Scandola, M.; Briese, B. H.; Jendrossek, D. *Macromolecules* **1996**, *29*, 507.

(11) Koyama, N.; Doi, Y. *Macromolecules* **1997**, *30*, 826.

(12) Abe, H.; Doi, Y.; Aoki, H.; Akehata, T. *Macromolecules* **1998**, *31*, 1791.

(13) Saracovan, I.; Keith, H. D.; Manley, R. St. J.; Brown, G. R. *Macromolecules* **1999**, *32*, 8918.

(14) Keith, H. D. *Polymer* **2001**, *42*, 9987.

(15) Galuska, A. A.; Poulter, R. R.; McElrath, K. O. *Surf. Interface Anal.* **1997**, *25*, 418.

(16) Tomasetti, E.; Nysten, B.; Legras, R. *Nanotechnology* **1998**, *9*, 305.

10.1021/la034865c CCC: $25.00
Published on Web 08/01/2003

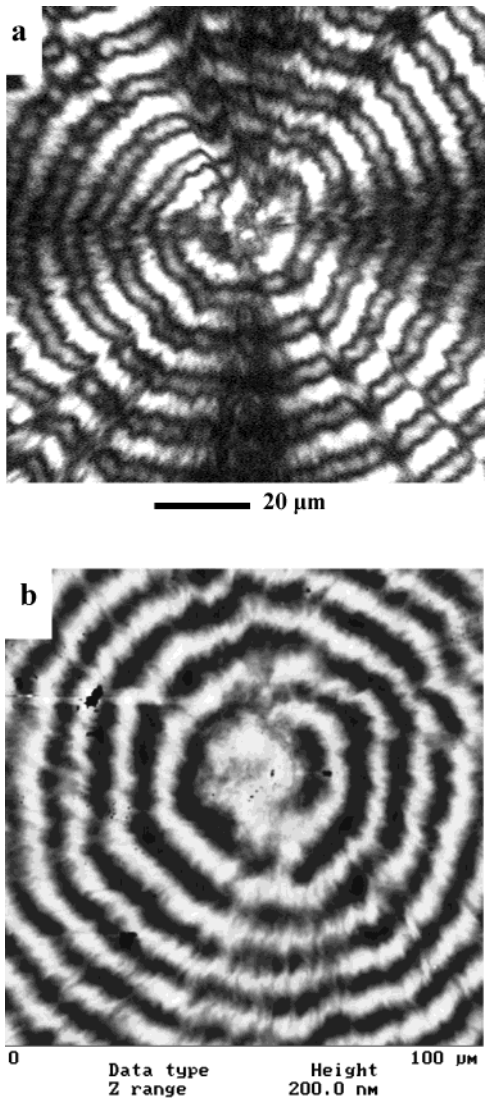

Figure 1. (a) Polarized optical micrograph of a banded spherulite of a P(3HB-3HV) film isothermally crystallized at 90 °C from the melt. (b) AFM height image of the same film obtained using tapping mode AFM.

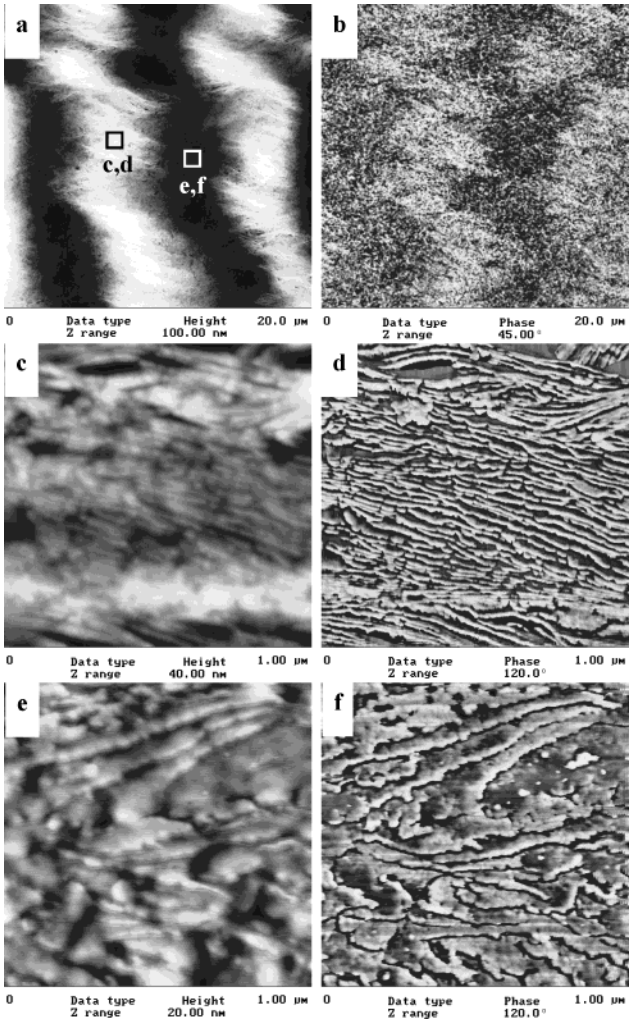

Figure 2. (a) and (b) AFM height and phase images showing several bands of a banded spherulite. (c) and (d) High-resolution AFM height and phase images showing edge-on lamellae at the ridges. (e) and (f) AFM height and phase images showing flat-on lamellae at the valleys.

measurement and force-volume imaging (FV)[20−24] have also been used to probe the local properties of the sample surfaces. Time-of-flight secondary ion mass spectrometry (ToF-SIMS) can provide detailed information on surface molecular structures,[25−26] including polymer tacticity,[27] sequence distribution,[28,29] end groups,[30] and the amounts of branching and cross-linking.[31] Moreover, the development of a time-of-flight analyzer allows the mapping of the surface chemical composition with a submicrometer resolution. The combined information of surface morphology and chemical composition is very useful to improve our understanding of the formation of banded spherulites and the degradation behavior of PHA films.

In this study, the surface morphology, the roughness, the frictional force, and adhesive force of poly(3-hydroxybutyrate-*co*-3-hydroxyvalerate) (P(3HB-3HV)) films were studied using AFM. The surface chemical composition was studied using ToF-SIMS. The relationships between the surface property, morphology, and chemical composition are presented.

Experimental Section

P(3HB-3HV) was synthesized by a microorganism as described in the literatures.[32−34] The glass transition temperature, melting

(17) Stroup, E. W.; Pungor, A.; Hlady, V. *Ultramicroscopy* **1996**, *66*, 237.
(18) VanLandingham, M. R.; McKnight, S. H.; Palmese, G. R.; Huang, X.; Bogetti, T. A.; Eduljee, R. F.; Gillepsie, J. W. *J. Adhes.* **1997**, *64*, 31.
(19) Burnham, N. A.; Kulik, A. J.; Oulevey, F.; Mayencourt, C.; Gourdon, D.; Dupas, E.; Gremaud, G. In *Micro/Nanotribology and Its Applications*; Bhushan, B., Ed.; NATO ASI Series E: Applied Sciences; Kluwer Academic Publishers: Dordrecht, 1997; No. 330, p 421.
(20) Reynaud, C.; Sommer, F.; Quet, C.; El Bounia, N..; Duc T. M. *Surf. Interface Anal.* **2000**, *30*, 185.
(21) Kim, D. T.; Blanch, H. W.; Radke, C. J. *Langmuir* **2002**, *18*, 5841.
(22) Walch, M.; Ziegler, U.; Groscurth, P. *Ultramicroscopy* **2000**, *82*, 259.
(23) Simpson, T. R. E.; Watts, J. F.; Zhdan, P. A.; Castlea, J. E.; Digby, R. P. *J. Mater. Chem.* **1999**, *9*, 2935.
(24) He, H. X.; Huang, W.; Zhang, H.; Li, Q. G.; Li, S. F. Y.; Liu, Z. F. *Langmuir* **2000**, *16*, 517.
(25) Reichlmaier, S.; Bryan, S. R.; Briggs, D. *J. Vac. Sci. Technol., A* **1995**, *13*, 1217.
(26) Weng, L. T.; Smith, T. L.; Feng, J.; Chan, C. M. *Macromolecules* **1998**, *31*, 928.
(27) Eynde X. V.; Weng, L. T.; Bertrand, P. *Surf. Interface Anal.* **1997**, *25*, 41.
(28) Galuska, A. A. *Surf. Interface Anal.* **1997**, *25*, 1.
(29) Zhuang, H. Z.; Gardella, J. A., Jr.; Hercules, D. M. *Macromolecules* **1997**, *30*, 1153.
(30) Affrossman, S.; Bertrand, P.; Hartshorne, M.; Kiff, T.; Leonard, D.; Pethrick, R. A.; Richards, R. W. *Macromolecules* **1996**, *29*, 5432.
(31) Lianos, L.; Quet, C.; Duc, T. M. *Surf. Interface Anal.* **1994**, *21*, 14.

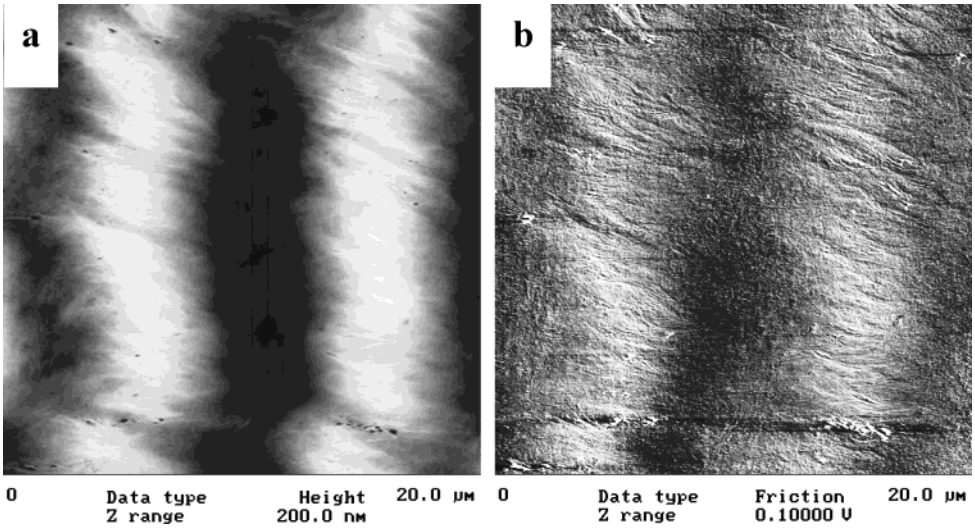

Figure 3. (a) and (b) AFM height and friction images of several bands of the spherulite.

point, weight-average molecular weight, and polydispersity index were measured to be approximately 2.5 °C, 150.2 °C, 60 800 g/mol, and 1.93, respectively. Banded spherulites were prepared by melting P(3HB-3HV) powder at 180 °C for 10 min and then transferring the sample onto a hot stage preset at 90 °C for isothermal crystallization.

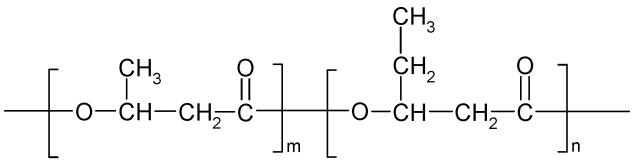

Chemical structure of the P(3HB-3HV)

Polarized optical images were obtained by a polarized optical microscope (POM) (Olympus BH-2) equipped with a hot stage (Leiz) and a CCD system (Panasonic 230). The surface morphology was recorded using a NanoScope IIIA MultiMode AFM (Digital Instruments) operating in the tapping mode at room temperature. Typical values for the set-point amplitude ratio varied from 0.7 to 0.9. Scan rates ranged from 0.8 to 1.0 Hz. Silicon tips (TESP, Digital Instruments) with a resonance frequency of approximately 300 kHz and a spring constant of about 40 $N \cdot m^{-1}$ were used. Roughness analysis was performed using AFM software (Digital Instruments) on the height image. LFM and FV imaging were performed in the contact mode. A 200-μm triangular silicon nitride cantilever (OTR8, Digital Instruments) with a nominal force constant of 0.15 $N\ m^{-1}$ was chosen to provide a large lateral deflection signal. The scan rate and the scan angle were set to 2.0 Hz and 90°, respectively, in the lateral force mode. Before an image was obtained, the procedure for force calibration for the AFM mode was used to minimize the contact force of the tip on the samples and to prevent sample damage. The force was kept constant for all the samples.

ToF-SIMS measurements were performed on a Physical Electronics PHI 7200 ToF-SIMS spectrometer. The chemical images of P(3HB-3HV) films were acquired in the negative mode using a $^{69}Ga^+$ liquid metal ion source operating at 25 keV. The mapped area was 150 μm × 150 μm with a maximum of 50 frame scans. The total ion dose was lower than 4×10^{11} ions/cm^2. The vacuum was about 1.5×10^{-9} Torr.

Results and Discussion

Figure 1a shows the polarized optical micrograph of a P(3HB-3HV) banded spherulite grown at 90 °C. When the sample was observed under light between crossed polarizers, alternating dark and bright concentric rings appeared in addition to a dark Maltese cross. It is well-known that the regular twisting of radial crystallite ribbons leads to the formation of a banded spherulite. Figure 1b shows the topography of a banded spherulite of the same film obtained using tapping-mode AFM. The surface of the banded spherulite is shown to consist of concentric ridges and valleys. A comparison of panels a and b of Figure 1 shows that the ridge surfaces in the AFM images correspond to the bright rings in the POM images. The width of the bands is approximately 10 μm, which is similar to the value measured by the POM. The average vertical distance between the ridges and valleys was measured to be about 120 nm.

High-resolution AFM images of the banded spherulite are shown in Figure 2. The bands appear to be irregular compared to those observed under POM because AFM images only show the morphology of the surface and the POM images obtained with transmitted light give the average lamellar orientation of the film. Panels c−f of Figure 2 show the detailed lamellar structure of the area marked by the squares in Figure 2a. Edge-on lamellae which are aligned parallel to each other can be clearly seen at the ridges, as shown in parts c and d of Figure 2. Flat-on lamellae can be observed in the valleys, as shown in parts e and f of Figure 2.

The surface roughness of the samples, shown in parts c and e of Figure 2, was estimated using AFM software, and the mean roughness (R_a) of an edge-on lamellar area (cf. Figure 2c) and a flat-on lamellar area (cf. Figure 2e) was measured to 3.1 and 1.5 nm, respectively. This difference in surface roughness may be caused by the difference in the lamellar orientation in these two areas. At the ridges, the lamellae were aligned in the edge-on orientation. The areas where the edge-on lamellae develop are expected to shrink, while the amorphous region which is sandwiched between two adjacent edge-on lamellae is expected to be higher than the crystalline regions. The corrugated structure may arise from the rough growth face. At the valleys, the lamellae were arranged in the flat-on orientation and the surface was covered by a very thin layer of loose loops and protruding cilia. Thus, it is very reasonable to find that the mean roughness at the ridges was larger than that of the valleys.

Figure 3 shows the height and friction images obtained in the lateral force mode. It can be seen that the ridge

(32) Findlay, R. H.; White, D. C. *Environ. Microbiol.* **1983**, *45*, 71.
(33) Park, C. H.; Damodaran, V. K. *Biotechnol. Bioeng.* **1994**, *44*, 1306.
(34) Koyama, N.; Doi, Y. *Biotechnol. Lett.* **1995**, *17*, 281.

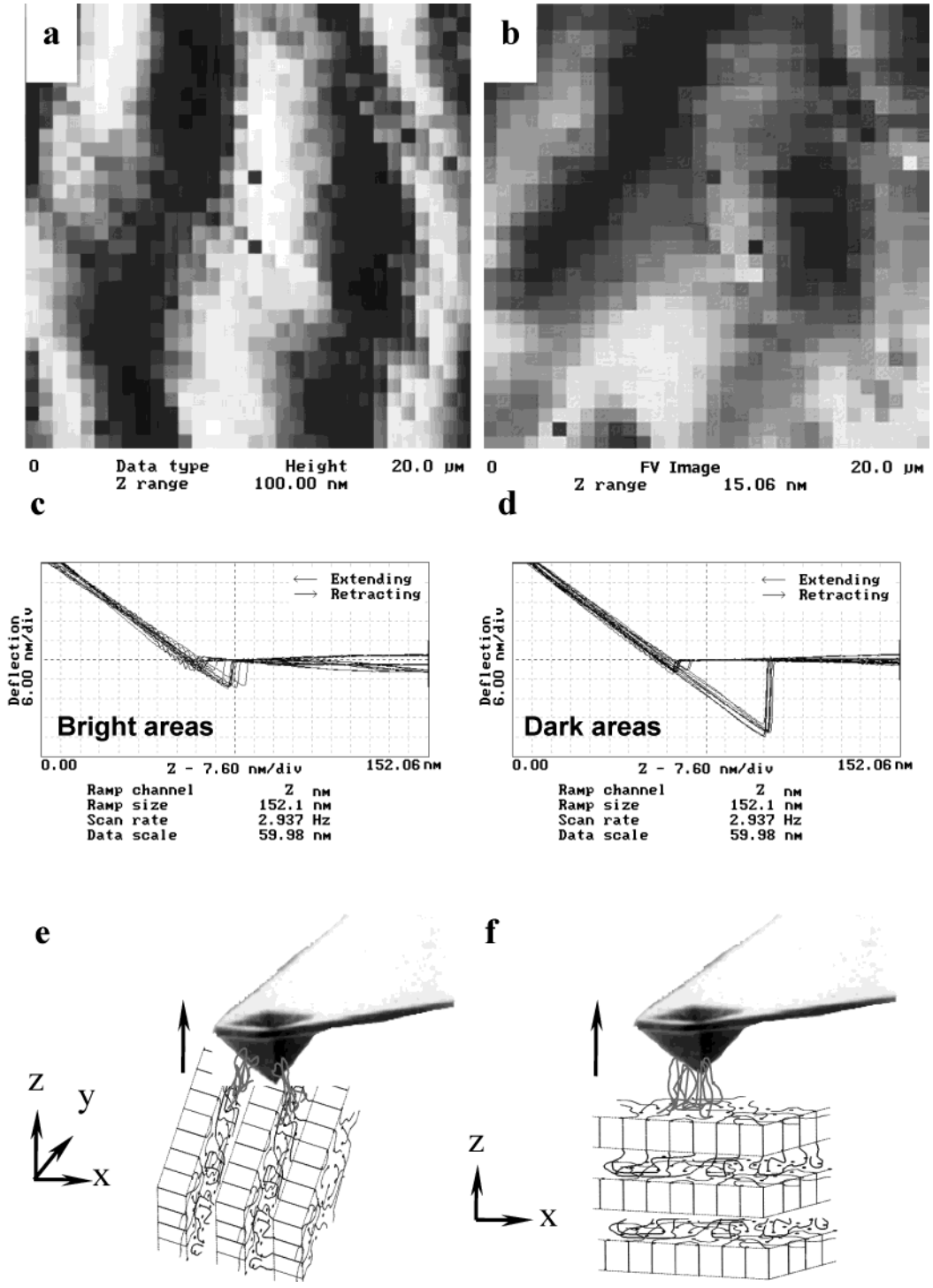

Figure 4. (a) and (b) AFM height and force−volume images observed in the force−volume mode. (c) and (d) Typical force−distance curves obtained respectively at the bright and dark areas shown in Figure 4b. (e) and (f) Schematic drawings of the interaction between the AFM probe and the edge-on and flat-on lamellae.

areas have a much large frictional force as shown in Figure 3b. Usually, the larger the roughness, the larger the frictional force. However, other effects, such as surface chemical composition, may also influence the frictional force between the AFM probe and the sample surface. Parts a and b of Figure 4 present the AFM height and FV images obtained using the AFM FV mode. With the adhesive interaction between the surface and the AFM probe monitored during the dissociation process, force curves can be obtained. The FV mode was performed by plotting the defection−distance curves across the sample surface at regular chosen intervals. For each $x-y$ pixel, the deflection versus the z-piezo displacement was recorded. A force−volume file includes three different types of information: the height image, the FV image, and the deflection−distance curves at each selected point. Figure 4a is the height image, which shows the topography of several bands of the spherulite. In Figure 4b, 32 defection−distance curves were recorded along each scanning line. Typical defection−distance curves at edge-on and flat-on lamellar areas are shown in parts c and d of Figure 4, respectively. The results show that small and large adhesive forces were detected in the ridges and valleys, respectively. At the ridge areas, where edge-on lamellae were present, the AFM tip was in contact with the growth face of the lamellae and the amorphous region which is

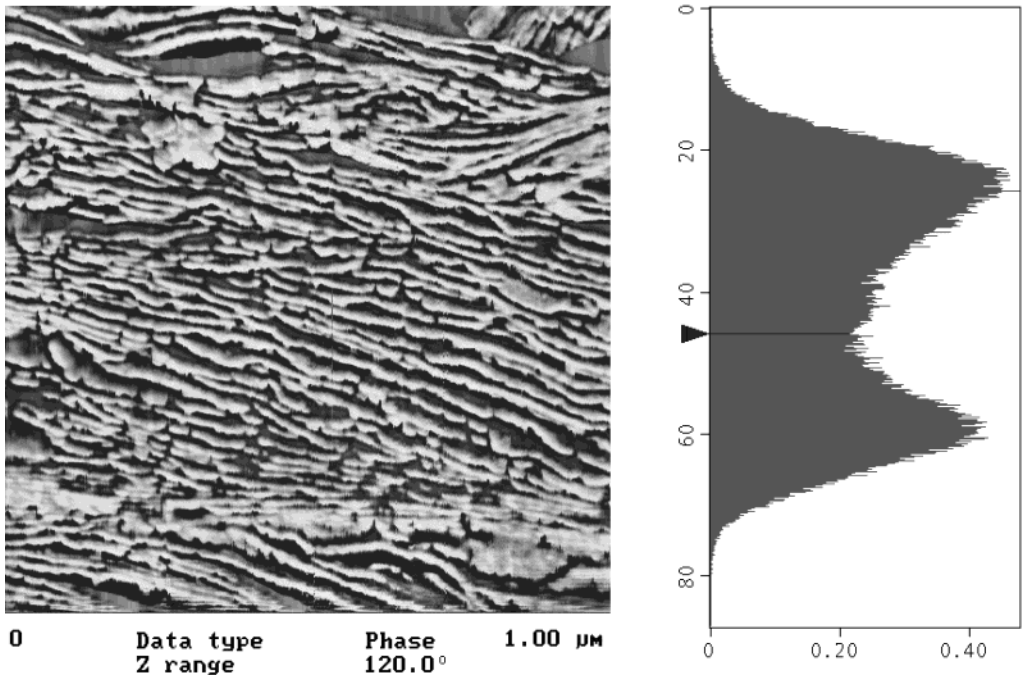

Figure 5. (a) AFM phase image and (b) bearing area percentage obtained by AFM on the edge-on lamellae at the ridges.

sandwiched between two adjacent edge-on lamellae. Considering that the polymer chain segments were folded regularly and parallel to the substrate at the edge-on lamellar region, the adhesive obtained by AFM might be mainly contributed by the interaction between AFM tip and the sandwiched amorphous region, as illustrated by Figure 4e. At the valley areas, where flat-on lamellae were present, the AMF tip was in contact with the folding surface of the lamellae. Usually, there were many loose loops and chain ends at the folding surface. When the AFM tip was withdrawn from the sample surface, the loops and chain ends at the folding surface could increase the adhesive interaction between AFM tip and sample surface, as shown in Figure 4f. The average adhesive force ratio of the edge-on lamellae to the flat-on one is about 0.35. The statistic ratio of the sandwiched amorphous regions to the surface area was estimated by AFM to be around 0.4, as shown in Figure 5. Therefore, the concentration of the loose loops and protruding cilia in the amorphous region, which is determined by the lamellar orientation, has shown to have a strong influence on the surface adhesive force.

Parts a and b of Figure 6 are the positive and negative ToF-SIMS chemical images of the area of a spherulite label with a square in Figure 6c, respectively. The periodic banded structures observed in the POM and ToF-SIMS chemical images are clearly related. To compare the peak intensities obtained from the ridges and the valleys, normalized peak intensities, I_i', which were calculated using eq 1 were used

$$I_i' = \frac{I_i}{\sum_i I_i} \tag{1}$$

where I_i is the intensity of the peak i. The ratios of the normalized intensities obtained from the ridge and valley were calculated and are summarized in Table 1. We can conclude that the surface chemical compositions of the ridges and valleys are very similar due to the fact that the ratios of the normalized intensities are very close to 1, as shown in Table 1. The variations in the peak intensity are caused by the difference in the surface topology of the ridges and valleys.

Our results show that AFM and ToF-SIMS can provide valuable information on surface structure and properties. It has been revealed that the rate of enzymatic hydrolysis of melt-crystallized PHA films decreased with the increase of crystallinity[9] and the average size of crystals.[10,12] However, Koyama and Doi[11] reported that the erosion rates of P(3HB-3HV) films were several times higher than the rates of P(3HB) homopolymer films with the same degree of crystallinity. The significant difference in the erosion rates for melt-crystallized films of P(3HB) homopolymer and P(3HB-3HV) copolymers could not be explained only in terms of the degree of crystallinity and the average size of the crystals. The enzymatic degradation behavior of single crystals of P(3HB) suggested that the single crystals were enzymatically hydrolyzed, preferentially at the crystal edges (*ac* plane) and ends (*bc* plane), rather than the chain-folding surfaces (*ab* plane) of the single crystals.[35−38] Moreover, two different types of planes were observed on the surface of P(3-hydroxybutyrate-*co*-6-hydroxyhexanoate) spherulites after enzymatic degradation, i.e., a smooth plane and a rough plane. These planes existed alternately along the radial direction of the spherulite.[12] From our observations, the smooth and the rough planes may consist of flat-on and edge-on lamellae, respectively. Our results show that surface properties, such as topography, rigidity, enzymatic erosion, roughness as well as the frictional and adhesive forces can be strongly affected by the lamellar orientations.

Conclusions

The surface properties of P(3HB-3HV) banded spherulites were studied using AFM and ToF-SIMS. The surface of the banded spherulite consists of ridges and valleys

(35) Iwata, T.; Doi, Y.; Kasuya, K.; Inoue, Y. *Macromolecules* **1997**, *30*, 833.
(36) Iwata, T.; Doi, Y.; Tanaka, T.; Akehata, T.; Shiromo, M.; Teramachi, S. *Macromolecules* **1997**, *30*, 5290.
(37) Nobes, G. A. R.; Marchessault, R. H.; Chanzy, H.; Briese, B. H.; Jendrossek, D. *Macromolecules* **1996**, *29*, 8330.
(38) Hocking, P. J.; Marchessault, R. H.; Timmins, M. R.; Lenz, R. W.; Fuller, R. C. *Macromolecules* **1996**, *29*, 2472.

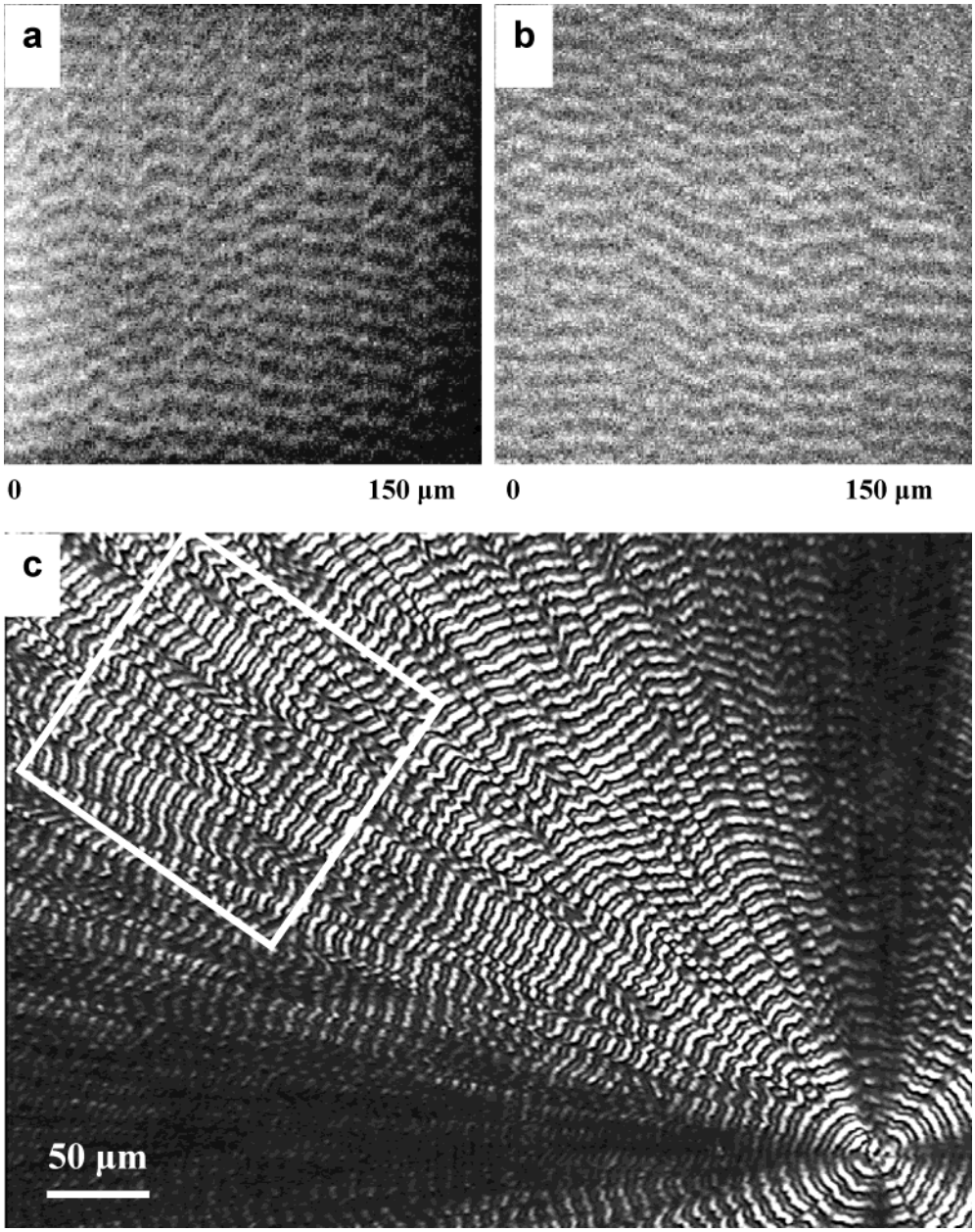

Figure 6. (a) and (b) positive and negative ToF-SIMS chemical images of the total ion intensity, respectively. (c) Polarized optical microscopy image.

Table 1. Ratios of the Normalized Peak Intensities Obtained from the Ridges and Valleys

m/z	positive ions	normalized intensity ratios (ridge/valley)	*m/z*	negative ions	normalized intensity ratios (ridge/valley)
15	CH_3^+	1.00	12	C^-	0.99
27	$C_2H_3^+$	0.93	13	CH^-	1.01
29	$C_2H_5^+$	0.97	14	CH_2^-	1.00
31	CH_3O^+	0.96	16	O^-	1.00
39	$C_3H_3^+$	1.06	17	OH^-	1.00
41	$C_3H_5^+$	0.98	24	C_2^-	1.05
43	$C_2H_3O^+$	0.96	25	C_2H^-	1.05
45	$C_2H_5O^+$	0.99	57	$C_3H_5O^-$	1.03
55	$C_4H_7^+$	0.99	59	$C_3H_7O^-$	1.07
59	$C_3H_7O^+$	0.99	85	$C_4H_5O_2^-$	1.08
69	$C_4H_5O^+$	1.00	87	$C_4H_7O_2^-$	1.06
87	$C_4H_7O_2^+$	0.97	99	$C_5H_7O_2^-$	0.90
101	$C_5H_9O_2^+$	0.99			

which were made up of edge-on and flat-on lamellae, respectively. The frictional force images showed that at the edge-on lamellar areas the interaction between the AFM probe and surface was larger than that at the flat-on lamellar areas. The adhesive force between the AFM probe at the edge-on lamellar areas was found to be much smaller than that at the flat-on lamellar areas. In addition, the surface chemical images obtained using ToF-SIMS show that the total intensities of the both positive and negative ions formed periodic patterns similar to those obtained using POM and AFM because of the surface topology of the banded spherulites. The ratios of the normalized peak intensities from the edge-on and flat-on lamellar areas were close to 1, implying that the surface chemical properties at these two areas were similar. Our results have shown that surface properties of semicrystalline polymers can be strongly influenced by the lamellar orientations.

Acknowledgment. We are grateful for the support of National Science Foundation of China (Grant No. 20044005, 20174049, and 20131160730) and the Hong Kong Government Research Grants Council under Grant No. N_HKUST 618/01.

LA034865C